

**Potential gradients produced by pore-space heterogeneities: Application to isothermal frost damage and submarine hydrate anomalies**

Alan W. Rempel<sup>1</sup> and Laura J. Van Alst<sup>2</sup>

<sup>1</sup>Department of Geological Sciences, University of Oregon, Eugene, OR 97401-1272; PH (541) 346-6316; FAX (541) 346-4692; email: rempel@uoregon.edu

<sup>2</sup>Sauder, Miller and Associates, 3451 Candelaria Road NE Ste. D, Albuquerque, NM 87107; lvanalst3@gmail.com

**ABSTRACT**

Deformation that results from crystallization in material pores commonly requires the supply of constituents through a fluid phase. With frost damage, the gradients in chemical potential necessary to drive transport are often caused by gradients in temperature. For submarine hydrates, compositional diffusion of methane is typically aligned with solubility gradients produced by the background temperature and pressure fields. Here, we show that under nearly isothermal and isobaric conditions, changes in the distribution of pore sizes can instead be the dominant cause of the potential gradients responsible for constituent supply. We illustrate the consequences and character of isothermal frost damage using the results from simple laboratory experiments. Field observations of hydrate anomalies in a submarine sand layer motivate comparison with a model for the diffusive growth of such deposits. These simple examples motivate further examination of the role of pore space heterogeneities in the development of other mineral systems.

**BACKGROUND**

Frost damage is a familiar consequence of the forces exerted during crystal growth in porous materials (Anderson, 1998; Hales and Roering, 2007; Hallet, 2006; Matsuoka and Murton, 2008; Murton, 2006; Washburn, 1980). At subzero temperatures, small amounts of liquid coexist in equilibrium with solid ice because of wetting interactions and surface-energy effects (e.g., Andersland and Ladanyi, 2004; Dash et al., 2006). Frost damage is caused by ice growth supplied with liquid that is driven down gradients in fluid pressure that parallel gradients in the temperature offset from bulk melting conditions (Walder and Hallet, 1985; Hallet et al., 1991). Hence, the common correlation between “freeze–thaw” cycles and degree of frost damage is understood to result from the increase in liquid supply during times when large temperature gradients connect thawed and ice-bound pores (Hallet, 2006). Laboratory experiments (Hallet et al., 1991; Murton, 2006), field observations (Hales and Roering, 2005; Matsuoka and Murton, 2008; Washburn, 1980) and theoretical predictions (Walder and

Hallet, 1985) have led to the concept of a “frost-cracking window” (Anderson, 1998) that is defined by the temperature regime in which most frost damage takes place. Damage requires subfreezing temperatures that are cold enough for wetting interactions between the ice and mineral surfaces to exert the pressures needed to propagate cracks, yet warm enough that the permeability to liquid flow is sufficient to supply the ice growth that enables crack extension. The liquid source is commonly associated with thawed regions, either nearer to the ground surface, or at greater depths (e.g. Hales and Roering, 2007). In contrast, here we describe how the extension of larger crack-like pores can also proceed under isothermal conditions as a type of “coarsening” process that is made possible by pore-space heterogeneities.

Pore-space heterogeneities can lead to the development of anomalous concentrations of crystalline constituents even when both pressure and temperature gradients are insignificant. For example, in layered submarine sediments, gas hydrates are commonly concentrated within the most coarse-grained material. Natural gas hydrates are crystalline “ices” that encapsulate methane within cages formed by hydrogen-bonded water molecules (Sloan and Koh, 2008). Anomalously high hydrate saturations in coarse-grained sediments have been attributed to both the influence of enhanced advective transport of dissolved methane along more permeable horizons (Boswell et al., 2012; Frye et al., 2012; Tréhu et al., 2004) and to a greater potential for larger pores to accommodate free gas bubbles that facilitate crystal nucleation (Kleinberg et al., 2003; Torres et al., 2008). However, recent modeling studies (Malinverno, 2010; Rempel, 2011) suggest that heterogeneous pore-size distributions may lead to anomalies in hydrate concentration even without the presence of either focussed fluid flow or free gas. Detailed bore hole and sediment core data from beneath the Gulf of Mexico (Cook and Malinverno, 2013) reveal high hydrate concentrations at both the upper and lower boundaries of a near-horizontal 2.5 m-thick sand layer, approximately 600 m above depths where the temperature is warm enough for free gas to be a stable phase, and adjacent to m-scale hydrate-free zones in the more fine-grained mud layers above and below. Over these short length-scales, temperature and pressure variations are minimal, and in any case are not oriented correctly to produce the gradients in dissolved gas concentration that are necessary to drive transport and establish both the upper and lower hydrate anomalies. Instead, simple models (Cook and Malinverno, 2013; Rempel, 2011) predict the growth of such anomalies as a consequence of changes in methane solubility with pore size and hydrate saturation level that result from wetting interactions and surface-energy effects.

These cases illustrate how pore-space heterogeneities produce gradients in the offset from bulk coexistence that drive material transport towards growing crystals. Although chosen for their simplicity and accessibility, both examples share essential features with more complicated mineral systems and remote geological environments. Veins of authigenic minerals have a rich variety of formation mechanisms; pore-space heterogeneities may contribute towards explaining the necessary material transport in some instances.

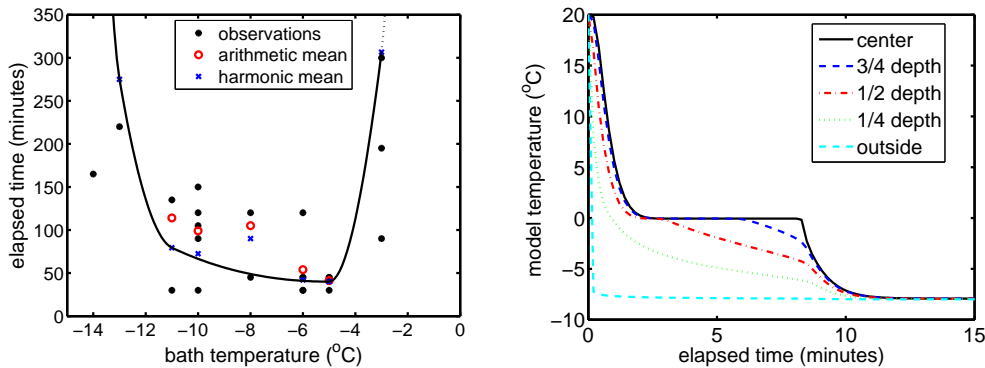


**Figure 1. Left: Time until visible frost damage in Eugene Formation sandstone cores immersed in an isothermal bath (van Alst, 2011). Right: Modeled temperature evolution at different radial positions within a 2.5 cm core immersed at  $-8^{\circ}\text{C}$ .**

### ISOTHERMAL FROST DAMAGE

In a series of step-freezing experiments, van Alst (2011) first observed frost damage at least 30–45 minutes after 2.5 cm-diameter, water-saturated sandstone cores were immersed in an isothermal bath at temperatures between  $-8^{\circ}\text{C}$  and  $-5^{\circ}\text{C}$ , whereas at warmer ( $\leq -2^{\circ}\text{C}$ ) or cooler ( $\geq -15^{\circ}\text{C}$ ) temperatures visible damage either required much more time or did not take place at all (see Fig. 1). This pattern of behavior was expected as a consequence of the dynamics responsible for the frost-cracking window discussed above. However, the delay until visible frost damage was much longer than the thermal diffusion time scale, and idealized calculations establish that only 10 minutes in the bath should have been sufficient to almost eliminate the temperature gradients that are normally held responsible for producing the gradients in liquid pressure that drive flow (see Fig. 1). These data require a mechanism for supplying continued crystal growth that propagates cracks while the cores are in an isothermal state.

Following Walder and Hallet (1985), a simple, yet illustrative model can be developed in which the porous rock is treated as an elastic solid that contains numerous, isolated crack-like pores. Within minutes after immersion in the cold bath, most of the pore liquid has frozen so that the stress intensity factor at the tip of a crack with radius  $a$  can be written as  $\sigma_I = \alpha\sqrt{a}(P_i - P_0)$ , where  $P_0$  is the background confining stress supported by the material far away,  $P_i$  is the pressure exerted by the ice against the pore walls, and  $\alpha$  is a geometrical parameter of order unity (e.g.  $\alpha = 2/\sqrt{\pi}$  for penny-shaped cracks (Gudmundsson, 2011)). Wetting interactions between the ice and pore walls cause the pressure  $P_l$  in an intervening liquid film to be depressed beneath  $P_i$  by an amount  $P_T = P_i - P_l$  that is the product of the depression beneath the bulk melting temperature  $T_m - T$  with the thermomolecular coefficient  $\rho L/T_m \approx 1.1 \text{ MPa/K}$  (e.g. Dash et al., 2006; Rempel et al., 2001), where  $\rho L$  is the volumetric latent heat of fusion

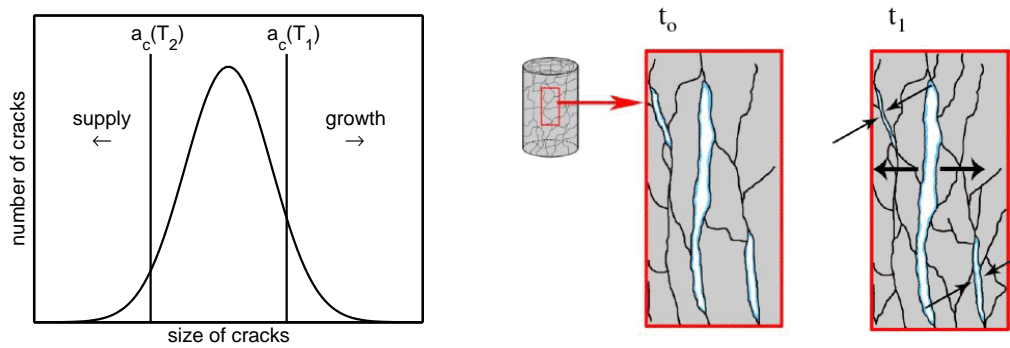


**Figure 2. Schematic depiction of the mechanism of isothermal frost damage. Left: Crack-size distribution with vertical lines illustrating the cutoff size for crack growth at two different temperatures. Right: As time progresses from  $t_0$  to  $t_1$ , larger cracks grow by pirating water away from smaller pores of size  $a < a_c$ .**

and  $T_m \approx 273$  K for ice. This implies that the stress intensity factor can be written as

$$\sigma_I = \alpha P_T \sqrt{a} \left( 1 - \frac{P_0 - P_l}{P_T} \right). \quad (1)$$

Crack growth is expected when  $\sigma_I$  exceeds a threshold  $\sigma_{Ic}$  that can be associated with the strength of the cement at grain contacts within the sandstone cores. Because  $P_T > 3$  MPa at temperatures below  $-3^\circ\text{C}$  where frost damage is observed (see Fig. 1), and the pressure difference  $P_0 - P_l$  in these experiments is expected to be less than 0.1 MPa, Eq. (1) predicts that  $\sigma_I > \sigma_{Ic}$  for pores that are larger than  $a_c(T) \approx [\sigma_{Ic}/(\alpha P_T)]^2$ . For example,  $a_c(-6^\circ\text{C})$  is a quarter the size of  $a_c(-3^\circ\text{C})$ , which corresponds with the smallest cracks that are expected to grow at the temperature where frost damage was first observed (see Fig. 1).

As the experiments demonstrate that significant frost damage occurs only long after isothermal conditions are established, the conceptual picture that emerges centers on the role of pore-scale heterogeneities (see Fig. 2). At a sufficiently cold temperature  $T_1 < T_m$ , wetting interactions are strong enough to promote the growth of crack-like pores that are larger than a threshold size  $a_c(T_1)$ . We expect crack extension to be accompanied by fluid flow and ice growth to fill the enlarged space, so the pressure  $P_l$  in the liquid coating the surfaces of larger cracks must drop to enable seepage transport from smaller pores with  $P_l \approx P_0$ . Eq. (1) predicts that the stress intensity factor  $\sigma_I$  is not significantly altered by changes in  $P_l$ , as long as they are limited to pressures that preclude cavitation so that  $P_l > 0$  (more precisely, the saturation vapor pressure in the confined space), and  $P_0 - P_l \ll P_T$ . For a particular distribution of initial crack sizes, there will be temperatures  $T > T_1$  that are too warm for any cracks to grow. At much colder temperatures  $T_2 < T_1$  the wetting forces along pore walls can become so strong that  $a_c(T_2)$  shrinks below the size of most cracks. Although more cracks are poised for growth at these colder temperatures, the water supply contained in smaller

pores is reduced correspondingly. Moreover, along the thin films that connect those pores small enough that  $\sigma_I < \sigma_{Ic}$  with the larger cracks that are able to extend and draw liquid flow, the decrease in permeability that accompanies the reduction in liquid volume slows the rate of frost damage to produce the pattern of behavior shown in Fig. 1 (van Alst, 2011). Frost damage by a coarsening mechanism of this nature might play a particularly important role during the evolution of landscapes in regions with thick permafrost that are characterized by shallow temperature gradients.

### SUBMARINE HYDRATE ANOMALIES

The methane solubility in an aqueous solution that is in contact with solid hydrate decreases with temperature and increases with pressure (Davie et al., 2004). On continental shelves where organic material is abundant, bacteria produce methane in sufficient concentrations for saturation to be reached so that hydrates form between the seafloor and a sediment depth that depends on the local geotherm and the hydrostatic load. On the Gulf of Mexico at Walker Ridge, for example, hydrates are stable to approximately 900 m below the seafloor “mbsf” (Cook and Malinverno, 2013). Beneath this level, dissolved methane concentrations reach saturation where free gas and an aqueous solution can coexist. Slow advective transport of dissolved methane can combine with in situ biogenic production to form massive hydrate deposits that constitute a significant fraction of global hydrocarbon reserves (e.g. Sloan and Koh, 2008).

Wetting interactions and surface-energy effects increase the methane solubility in porous media. For example, with pores of characteristic radius  $a$ , when the volume fraction of hydrate in the pore space is  $S_h$ , at temperature  $T$  and pressure  $P$ , the solubility can be approximated by (cf. Rempel, 2011, Eq. 14)

$$c_{eq}(a, S_h) \approx c_0(T, P) \left[ 1 + \frac{2\gamma(1 - S_h)^{-1/\beta}}{a\alpha_s(\rho L/T)} \right], \quad (2)$$

where  $c_0(T, P)$  is the solubility in the absence of sediment interactions,  $\gamma \approx 0.035 \text{ J/m}^2$  is the surface energy of the hydrate–liquid interface,  $\alpha_s \approx 14.4 \text{ K}$  for typical geothermal gradients (Davie et al., 2004), the thermomolecular coefficient for hydrate is  $\rho L/T \approx 1.4 \text{ MPa/K}$ , and the empirical constant  $\beta \approx 1.3$  varies modestly with changes in the distribution of pore-sizes about the mean (e.g., Rempel, 2012). For example, Eq. (2) predicts that with  $S_h \ll 1$  the solubility in pores of radius  $10 \mu\text{m}$  is approximately 0.035% greater than  $c_0$ , and the solubility in pores of radius  $1 \mu\text{m}$  is 0.35% greater than  $c_0$ . Although these solubility differences are very small, since diffusion requires that the dissolved concentration remain continuous across stratigraphic boundaries, hydrate anomalies can grow in coarse-grained sediments adjacent to hydrate-free regions in more fine-grained muds.

The left side of Fig. 3 shows  $S_h$  inferred from well-log resistivity data at Walker Ridge Hole 313-H (Cook and Malinverno, 2013). The prominent double spike in hydrate saturation is mimicked (though diminished in magnitude) on the right by a sim-

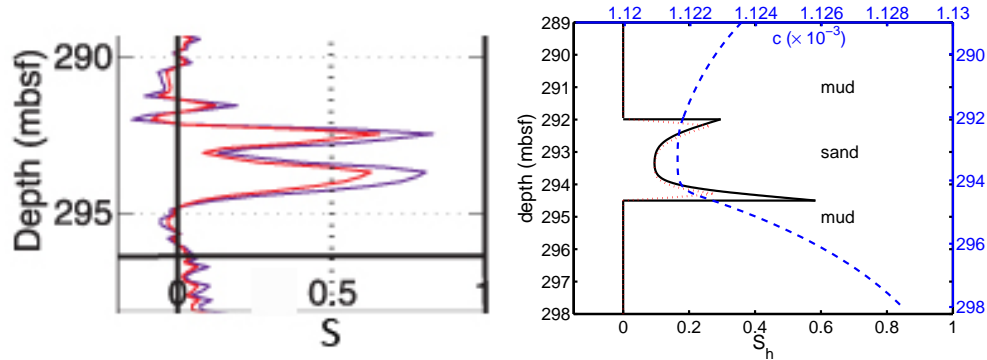


**Figure 3. Left: Estimates of hydrate saturation in well log data (modified from Cook and Malinverno, 2013). Right: Model calculations for hydrate accumulation in a sandy layer adjacent to muds with 10 times finer grain size. Solid line is modeled  $S_h$ , dotted is a running average of  $S_h$ , dashed is dissolved gas concentration.**

ple model after Rempel (2011), that considers a 2.5 m thick sand layer with pores that are an order of magnitude larger than the mud layers on either side. The one-dimensional treatment demonstrates how diffusive transport down the concentration gradient (dashed line on the right in Fig. 3) causes anomalies to develop in the coarse-grained sediments at stratigraphic boundaries by concentrating the hydrate that would otherwise have accumulated in the hydrate-free regions of adjacent fine-grained material (Rempel, 2011). For a scenario involving 1 and 10  $\mu\text{m}$  pores, Eq. (2) predicts that hydrates only become stable in the fine-grained sediments once the hydrate saturation in the more coarse-grained sediments reaches  $S_h \approx 1 - (1 \mu\text{m}/10 \mu\text{m})^\beta \approx 95\%$ . For the model calculations shown on the right side of Fig. 3, the mud remains hydrate-free for 3.6 m below the sand layer and 6.2 m above, compared to well-log observations of 3.2 m and 10.3 m hydrate-free regions in Hole 313-H (Cook and Malinverno, 2013). The modeled large-scale methane supply comes from vertical Darcy transport at 4 mm/a over 400 ka assuming a gas-saturated source 600 m below the sand layer at the base of the hydrate stability zone and a geothermal gradient of 0.025 K/m; since the resulting methane flux is insufficient to fully capture the magnitude of the observed anomalies, this suggests an important role for nearby methanogenesis, consistent with mass-balance calculations discussed further by Cook and Malinverno (2013). Far away from the sand layer in the fine-grained muds, hydrate forms in prominent cracks that are reminiscent of ice lenses and mineral veins.

**DISCUSSION AND CONCLUSIONS**

The examples above illustrate how pore space heterogeneities influence crystallization in simple systems. More broadly, veins of authigenic minerals have been attributed to a spectrum of formation mechanisms, with differing explanations for the required constituent transport, and creation of the necessary space (e.g. Bons, 2001;

Breeding and Ague, 2002; Ferry and Dipple, 1991; Ramsay, 1980; Wangen and Munz, 2004). One end-member class of models relies upon the forces that growing crystals exert on the host rock to make space (Fletcher and Merino, 2001; Wiltshko and Morse, 2001) in much the same way as for the frost-damage case discussed above. Pseudomorphic transitions in which minerals are replaced in coupled diffusion–precipitation reactions have been suggested to proceed either as a result of the dissolving phase contributing to supersaturation of the precipitating phase, or because the force of crystallization enables local supersaturation in confined spaces (Maliva and Siever, 1988; Putnis, 2009). Detailed analyses of rims on crystals grown in confined spaces have been interpreted as evidence for frost-damage-like behavior (Røyne and Dysthe, 2012). Similar thermodynamic and mechanical considerations have been suggested to control the formation of travertine veins in some mineral-springs environments (Gratier et al., 2012). Pore-size controls on solubility (Emmanuel and Berkowitz, 2007) should enable minerals to precipitate in segregated forms adjacent to more fine grained material that is free of the precipitate (Emmanuel et al., 2010), much as is seen in the gas hydrate deposits discussed above (Cook and Malinverno, 2013; Rempel, 2011).

The potential gradients that are necessary for the growth of crystals in confined spaces are often associated with gradients in the imposed state variables, such as temperature or fluid pressure. When wetting interactions and surface-energy effects are important, changes in pore geometry are another potential cause of material transport. Frost damage and marine hydrate anomalies are simple illustrations of the physical consequences. The broader influence of similar dynamic interactions in other mineral systems awaits further investigation.

## REFERENCES

- Andersland, O. B., and Ladanyi, B. (2004). *An Introduction to Frozen Ground Engineering*, 363 pp., Chapman and Hall, New York.
- Anderson, R.S. (1998). “Near-surface thermal profiles in alpine bedrock: Implications for the frost weathering of rock.” *Arc. Alpine Res.*, 30(4), 362–372.
- Bons, P.D. (2001). “The formation of large quartz veins by rapid ascent of fluids in mobile hydrofractures”. *Tectonophys.*, 336(1), 1–17.
- Boswell, R., Collett, T.S., Frye, M., Shedd, W., McConnell, D.R., and Shelander, D. (2012). “Subsurface gas hydrates in the northern Gulf of Mexico.” *Mar. Pet. Geol.*, 34(1), 4–30, doi: 10.1016/j.marpetgeo.2011.10.003.
- Breeding, C.M., and Ague, J.J. (2002). “Slab-derived fluids and quartz-vein formation in an accretionary prism, Otago schist, New Zealand”. *Geology*, 30(6), 499–502.
- Cook, A.E., and Malinverno, A. (2013). “Short migration of methane into a gas hydrate-bearing sand layer at Walker Ridge, Gulf of Mexico.” *G-Cubed*, in press.

- Dash, J. G., Rempel, A. W., and Wettlaufer, J. S. (2006). "The physics of premelted ice and its geophysical consequences." *Rev. Mod. Phys.*, 78, 695–741.
- Davie, M. K., O. Y. Zatsepina, and Buffett, B.A. (2004). "Methane solubility in marine hydrate environments." *Mar. Geol.*, 203, 177–184.
- Dickens, G. R., M. M. Castillo, and Walker, J.C.G. (1997). "A blast of gas in the latest Paleocene: Simulating first-order effects of massive dissociation of oceanic methane hydrate", *Geology*, 25, 259–262.
- Emmanuel, S., and Berkowitz, B. (2007). "Effects of pore-size controlled solubility on reactive transport in heterogeneous rock". *Geophys. Res. Lett.*, 34(6), L06404.
- Emmanuel, S., Ague, J.J., and Walderhaug, O. (2010). "Interfacial energy effects and the evolution of pore size distributions during quartz precipitation in sandstone". *Geochim. Cosmochim. Acta*, 74(12), 3539–3552.
- Ferry, J.M., and Dipple, G.M. (1991) "Fluid flow, mineral reactions, and metasomatism". *Geology*, 19(3), 211–214.
- Fletcher, R.C., and Merino, E. (2001). "Mineral growth in rocks: Kinetic-rheological models of replacement, vein formation, and syntectonic crystallization". *Geochim. Cosmochim. Acta*, 65(21), 3733–3748.
- Frye, M., Shedd, W. and Boswell, R. (2012). "Gas hydrate resource potential in the Terrebonne Basin, Northern Gulf of Mexico." *Mar. Pet. Geol.*, 34(1), 150-168, doi: 10.1016/j.marpetgeo.2011.08.001.
- Gratier, J.P., Frery, E., Deschamps, P., Røyne, A., Renard, F., Dysthe, D., Ellouz-Zimmerman, N., and Hamelin, B. (2012). "How travertine veins grow from top to bottom and lift the rocks above them: The effect of crystallization force". *Geology*, doi:10.1130/G33286.1.
- Gudmundsson, A. (2011). *Rock Fractures in Geological Processes*, Cambridge, New York, 578 pp.
- Hales, T. C., and Roering, J.J. (2005). "Climate-controlled variations in scree production, Southern Alps, New Zealand." *Geology*, 33(9) 701–704.
- Hales, T. C., and Roering, J.J. (2007). "Climatic controls on frost cracking and implications for the evolution of bedrock landscapes." *J. Geophys. Res.*, 112, F02033, doi:10.1029/2006JF000616.
- Hallet, B. (2006). "Why do freezing rocks break?" *Science*, 314, 1092–1093.
- Hallet, B., Walder, J. S., and Stubbs, C. W. (1991). "Weathering by segregation ice growth in microcracks at sustained sub-zero temperatures: Verification from an experimental study using acoustic emissions." *Permafrost Periglacial Proc.*, 2, 283–300.
- Kleinberg, R. L., C. Flaum, D. D. Griffin, P. G. Brewer, G. E. Malby, E. T. Peltzer, and J. P. Yesinowski. (2003). "Deep sea NMR: Methane hydrate growth habit

- in porous media and its relationship to hydraulic permeability, deposit accumulation, and submarine slope stability." *J. Geophys. Res.*, 108(B10), 2508, doi:10.1029/2003JB002389.
- Malinverno, A. (2010). "Marine gas hydrates in thin sand layers that soak up microbial methane." *Earth Plan. Sci. Lett.*, 292, 399–408.
- Maliva, R.G., and Siever, R. (1988). "Diagenetic replacement controlled by force of crystallization". *Geology*, 16(8), 688–691.
- Matsuoka, N., and Murton, J. (2008). "Frost weathering: Recent advances and future directions." *Permafrost Periglacial Proc.*, 19, 195–210.
- Murton, J. B., Peterson, R., and Ozouf, J.-C. (2006). "Bedrock fracture by ice segregation in cold regions." *Science*, 314, 1127–1129.
- Putnis, A. (2009). "Mineral replacement reactions". *Rev. Mineral. Geochem.*, 70(1), 87–124.
- Ramsay, J.G. (1980). "The crack-seal mechanism of rock deformation". *Nature*, 284, 135–139,
- Rempel, A.W. (2011). "A model for the diffusive growth of hydrate saturation anomalies in layered sediments." *J. Geophys. Res.*, 116, doi:10.1029/2011JB008484.
- Rempel, A.W. (2012). "Hydromechanical processes in freezing soils." *Vadose Zone J.*, 11, doi:10.2136/vzj2012.0045.
- Rempel, A. W., Wettlaufer, J. S., and Worster, M. G. (2001). "Interfacial premelting and the thermomolecular force: Thermodynamic buoyancy." *Phys. Rev. Lett.*, 87, 088501.
- Røyne, A., and Dysthe, D.K. (2012). "Rim formation on crystal faces growing in confinement". *J. Crystal Growth*, 346(1), 89–100.
- Sloan, E.D., and Koh, C.A. (2008). *Clathrate Hydrates of Natural Gases*, 3rd ed., CRC Press, Boca Raton, 721 pp.
- Torres, M. E., Tréhu, A.M., Cespedes, N., Kastner, M., Wortmann, U.G., Kim, J.-H., Long, P., Malinverno, A., Pohlman, J.W., Riedel, M., and Collett, T. (2008). "Methane hydrate formation in turbidite sediments of northern Cascadia IODP Expedition 311." *Earth Plan. Sci. Lett.*, 271, 170–180.
- Tréhu, A. M., Flemings, P.B., Bangs, N.L., Chevallier, J., Gràcia, E., Johnson, J.E., Liu, C.-S., Liu, X., Riedel, M., and Torres, M.E. (2004). "Feeding methane vents and gas hydrate deposits at south Hydrate Ridge." *Geophys. Res. Lett.*, 31, L23301, doi:10.1029/2004GL021286.
- van Alst, L.J. (2011). *Laboratory experiments in cold temperature rock deformation*. MSc thesis, University of Oregon, <http://hdl.handle.net/1794/12191>.
- Walder, J., and Hallet, B. (1985). "A theoretical model of the fracture of rock during freezing." *Geol. Soc. Am. Bull.*, 96, 336–346.

- Wangen, M., and Munz, I.A. (2004). "Formation of quartz veins by local dissolution and transport of silica". *Chem. Geol.*, 209(3), 179–192.
- Washburn, A. L. (1980). *Geocryology*. Halstead Press. New York. 406 pp.
- Wiltchko, D.V., and Morse, J.W. (2001). "Crystallization pressure versus crack seal as the mechanism for banded veins". *Geology*, 29(1), 79–82.